

## Research Paper

## 2-O- $\beta$ -D-glucopyranosyl-L-ascorbic acid, a novel vitamin C derivative from *Lycium barbarum*, prevents oxidative stress

Shen-Fei Wang<sup>a</sup>, Xin Liu<sup>a</sup>, Mo-Yu Ding<sup>a</sup>, Shuangcheng Ma<sup>a,b</sup>, Jing Zhao<sup>a,\*\*\*</sup>, Ying Wang<sup>a,\*</sup>, Shaoping Li<sup>a,\*,\*\*</sup>

<sup>a</sup> Institute of Chinese Medical Sciences and State Key Laboratory of Quality Research in Chinese Medicine, University of Macau, Avenida da Universidade, Taipa, Macao SAR, China

<sup>b</sup> National Institutes for Food and Drug Control, Beijing, 100050, China



## ARTICLE INFO

## Keywords:

Ascorbic acid  
2-O- $\beta$ -D-glucopyranosyl-L-ascorbic acid (AA-2 $\beta$ G)  
Oxidative stress  
*Lycium barbarum*  
Nuclear factor E2-related factor 2 (Nrf2)

## ABSTRACT

Reducing agents are crucial for the management of maladaptive inflammation-induced macrophage death and hematopoietic toxicity of chemotherapy. 2-O- $\beta$ -D-glucopyranosyl-L-ascorbic acid (AA-2 $\beta$ G), a unique AA (or vitamin C) derivative identified in *Lycium barbarum*, exhibited enhanced free radical scavenging activity compared with AA and its synthetic derivative AA-2 $\alpha$ G. AA-2 $\beta$ G protected hydrogen peroxide-induced cell death in murine macrophage RAW264.7 cells. Treatment with AA-2 $\beta$ G eliminated oxidative stress and the ratio of cellular glutathione to glutathione disulfide more effectively than AA and AA-2 $\alpha$ G. AA-2 $\beta$ G also significantly reduced the fluorescent intensity of DCFH-DA triggered by chemotherapeutic agent camptothecin-11 but not fluorouracil. AA, AA-2 $\alpha$ G, and AA-2 $\beta$ G significantly decreased Keap-1 expression, and increased the expression levels of nuclear factor E2-related factor 2 (Nrf2) and heme oxygenase-1. All compounds triggered the nuclear translocation of Nrf2, while the ability of AA-2 $\beta$ G to enhance the Nrf2-DNA binding affinity was approximately two fold as those of AA and AA-2 $\alpha$ G. Sodium ascorbate cotransporters (SVCT) inhibitors, sulfinpyrazone, phloretin, and 3-O-methylglucose, potentially abrogated the free radical scavenging activities of AA, AA-2 $\alpha$ G, and AA-2 $\beta$ G. The cellular uptake efficacy of AA-2 $\alpha$ G and AA-2 $\beta$ G was less than 10% of AA, while the inhibition of SVCT with sulfinpyrazone considerably diminished the uptake efficacy of these compounds. AA-2 $\alpha$ G and AA-2 $\beta$ G are more stable in the Fenton reagents than AA. In summary, AA-2 $\beta$ G from *L. barbarum* with excellent free radical scavenging activity is a promising natural AA derivative for further pharmacological evaluation.

## 1. Introduction

Imbalance between the oxidant and antioxidant system results in excess amounts of free radicals and hence oxidative stress (ROS), which is considered as a two-edged weapon. The accumulation of free radicals is associated with maladaptive inflammation-induced macrophage death that leads to the subsequent necrotic death of plaque cells [1]. Chronic elevated ROS is also responsible for hematopoietic toxicity of chemotherapeutic agents [2] and the development of many types of diseases, including various types of cancer [3] and neurodegenerative diseases [4]. Meanwhile, exclusive generation of intracellular free radicals, such as hydrogen peroxide (H<sub>2</sub>O<sub>2</sub>) and superoxide (O<sub>2</sub><sup>-</sup>), through the oxidation of antioxidants induces apoptotic cell death in KRAS and BRAF mutant colorectal cancer [5,6]. Therefore, the pursuit of potent antioxidant reagents for pharmacological use continues.

L-Ascorbic acid (AA, or vitamin C, Fig. 1A) is one of the most widely used antioxidant in the food and cosmetic industry [5,6]. However, AA is easily oxidized to dehydrated AA (DHA) in aqueous solution [5,7]. The pharmacological but not physiology dose of AA increases the risk of kidney stone, and renal and metabolic toxicity [8]. Therefore, stable AA derivative with fast and long-lasting free radical scavenging activity and reduced therapeutic dose is urgently needed.

Medicinal plants are a rich source of antioxidants. Solanaceae family plants *Lycium barbarum* and *L. chinense* have been used as traditional Chinese Medicine for over 2,000 years [9]. The ripe fruits of *L. barbarum* and *L. chinense* or wolfberry are used to prevent or treat several types of diseases. The properties of these fruits include benefits on complexion and maintaining of beauty according to the "Compendium of Materia Medica" [10], as well as maintenance of vision [11], kidney, and liver functions [9]. Wolfberry is used as a tonic herb and functional food with antioxidant [12],

\* Corresponding author.

\*\* Corresponding author.

\*\*\* Corresponding author.

E-mail addresses: [Jingzhao@um.edu.mo](mailto:Jingzhao@um.edu.mo) (J. Zhao), [emilywang@um.edu.mo](mailto:emilywang@um.edu.mo) (Y. Wang), [spli@um.edu.mo](mailto:spli@um.edu.mo) (S. Li).

<https://doi.org/10.1016/j.redox.2019.101173>

Received 1 January 2019; Received in revised form 9 March 2019; Accepted 15 March 2019

Available online 18 March 2019

2213-2317/© 2019 The Authors. Published by Elsevier B.V. This is an open access article under the CC BY license (<http://creativecommons.org/licenses/by/4.0/>).

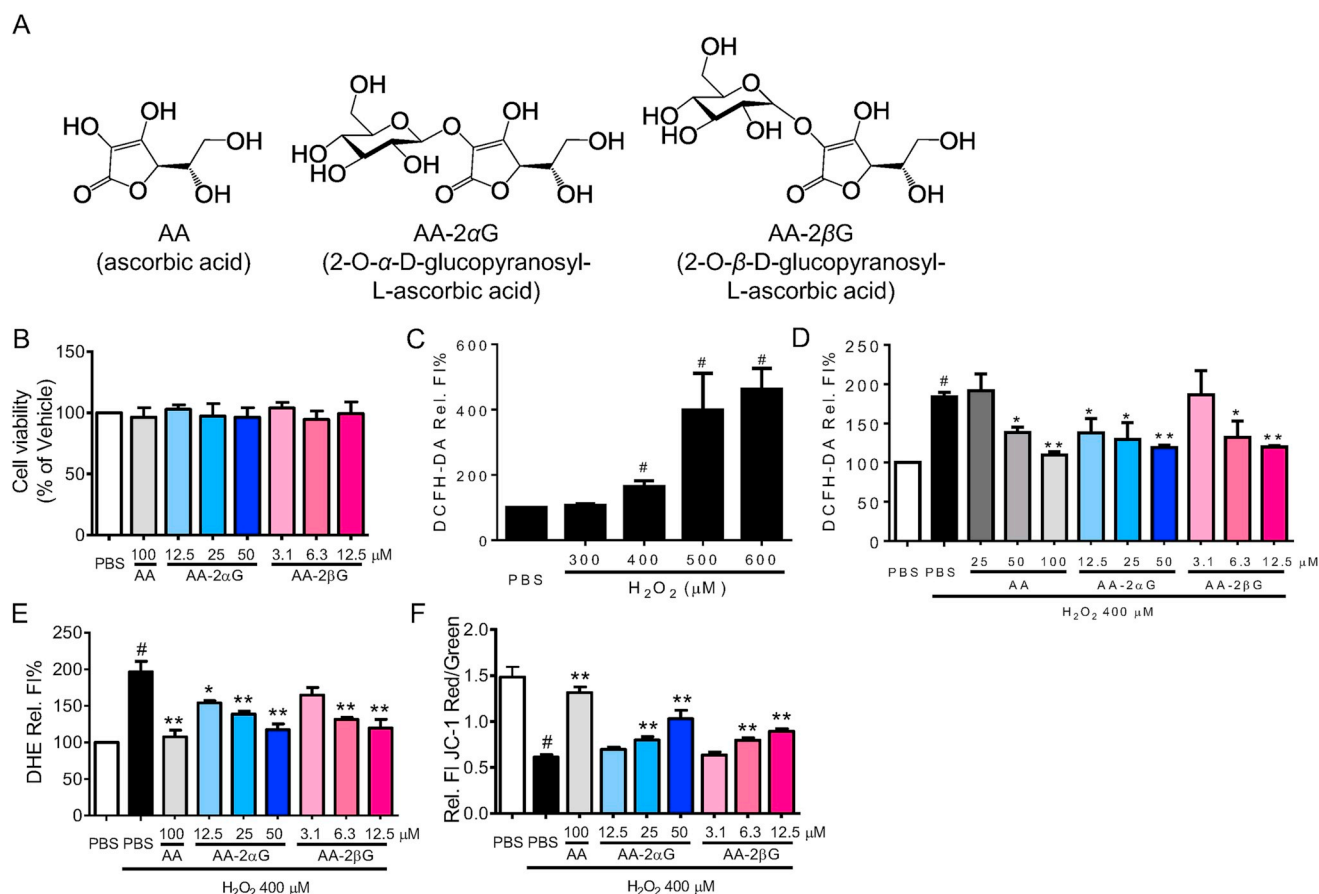


**Fig. 1.** Treatment with AA, AA-2αG, and AA-2βG prevented H<sub>2</sub>O<sub>2</sub>-induced cell death in RAW264.7 cell. (A) Chemical structures of AA, AA-2αG, and AA-2βG. (B) RAW264.7 cell viability was measured by MTT assay after treatment with different AA, AA-2αG, and AA-2βG concentrations for 4 h. (C) RAW264.7 cells were treated with different H<sub>2</sub>O<sub>2</sub> dosages of for 30 min. The H<sub>2</sub>O<sub>2</sub>-stimulated ROS generation was measured by DCFH-DA staining. RAW264.7 cells were pretreated with different f AA, AA-2αG, and AA-2βG concentrations for 1 h, followed by H<sub>2</sub>O<sub>2</sub> treatment for another 30 min. Generation of ROS was analyzed by (D) DCFH-DA and (E) DHE staining, and (F) the effect on mitochondrial transmembrane potential was measured using JC-1 staining. The results are presented as mean ± SD from three separate experiments (\*,  $p < 0.05$  and \*\*,  $p < 0.01$  compared with H<sub>2</sub>O<sub>2</sub> treatment; #,  $p < 0.05$  compared with PBS treatment).

anti-inflammation [13], and antiaging activities [14]. Phenolics [15], *L. barbarum* polysaccharides, β-carotenoids [16,17], or flavonoids [18] isolated from wolfberry exhibit potent radical scavenging activities. A novel AA derivative, 2-O-β-D-glucopyranosyl-L-AA (AA-2βG, Fig. 1A), was first purified from *L. barbarum* by Toyoda-Ono et al. in 2004 [19]. AA-2βG exhibited comparable antioxidant activities to AA and its synthetic derivative 2-O-α-D-glucopyranosyl-L-AA (AA-2αG, Fig. 1A) in cell-free 1,1-diphenylpicrylhydrazyl radical scavenging assay [20,21]. AA-2βG downregulates the serum aspartate transaminase and alanine aminotransferase levels in carbon tetrachloride-induced murine hepatic damage model [22]. A comparative analysis of the radical scavenging activity and the mechanisms of action of AA, AA-2αG, and AA-2βG have not been conducted yet.

In the present study, we mainly evaluated the ROS scavenging potentials of AA, AA-2αG, and AA-2βG in M1/M2-like murine macrophage RAW264.7 cells. We also determined the effect of the D-glucosyl moiety and its configuration on cellular uptake and molecular mechanism. Our results provided the first pharmacological evidence that AA-2βG, the novel and stable AA derivative from *L. barbarum*, with enhanced free radical scavenging activity.

## 2. Materials and methods

### 2.1. Materials and reagents

H<sub>2</sub>O<sub>2</sub> was purchased from Aladdin (Shanghai, China). Fluorescent probe 2',7'-dichlorofluorescein diacetate (DCFH-DA), dihydroethidium

(DHE), 5,5',6,6'-tetrachloro-1,1',3,3'-tetraethylbenzimidazolylcarbocyanine iodide (JC-1), AA, AA-2αG, camptothecin-11 (CPT-11), 5-fluorouracil (5-FU), and 3-O-methylglucose were obtained from Sigma-Aldrich (St. Louis, MO, USA). AA-2βG was separated and purified as previously reported [21]. Sodium-ascorbate co-transporters (SVCT) and glucose transporter inhibitors sulfinpyrazone (SU), phloretin (PH), and 3-O-methyl glucose (3-OMG) were purchased from Cayman Chemical (Ann Arbor, MI, USA). Phosphate-buffered saline (PBS), Dulbecco's modified Eagle medium (DMEM), fetal bovine serum (FBS), and 100 × penicillin and streptomycin were purchased from Gibco-Invitrogen (Paisley, Scotland, UK). AA-2αG and AA-2βG were dissolved in PBS prior to use. Superoxide dismutase (SOD), catalase (CAT), glutathione (GSH), and glutathione disulfide (GSSG) detection kits were purchased from Beyotime Biotechnology (Shanghai, China).

### 2.2. Cell culture and treatment condition

Murine macrophage RAW 264.7 cell line was acquired from the American Type Culture Collection (ATCC, Rockville, MD, USA), and cultured in DMEM medium supplemented with 10% fetal bovine serum, 100 U/mL penicillin and streptomycin with humidified atmosphere of 5% CO<sub>2</sub> at 37 °C.

For detection of SOD, CAT, GSH, GSSG, DHL, TNF-α, and western blot analysis, RAW264.7 cells were pre-incubated with AA, AA-2αG, or AA-2βG for 4 h, and then stimulated with 400 μM H<sub>2</sub>O<sub>2</sub> for 6 h.

For co-treatment with SVCT inhibitors, RAW264.7 cells were pre-

incubated with 5  $\mu\text{M}$  SU, 10  $\mu\text{M}$  PH, or 10  $\mu\text{M}$  3-OMG for 20 min and pre-treated with AA, AA-2 $\alpha$ G, or AA-2 $\beta$ G for 4 h. ROS was then stimulated with 400  $\mu\text{M}$  H<sub>2</sub>O<sub>2</sub> for 30 min.

### 2.3. Cell viability assay

RAW 264.7 cells were seeded in 96 well plates for 18 h and then treated with AA, AA-2 $\alpha$ G, AA-2 $\beta$ G, or PBS as vehicle for 4 h. MTT was then added at 5 mg/mL for an addition 4 h at 37 °C. At the end of the incubation, the formazan crystals were dissolved with DMSO. The absorbance was determined at 570 nm using MultiLabel Counter Victor (PerkinElmer, Waltham, MA, USA). Cell viability was calculated by the ratio of absorbance between treated and vehicle groups.

### 2.4. Detection of ROS and mitochondrial transmembrane potential ( $\Delta\Psi\text{m}$ )

For ROS detection, RAW 264.7 cells were pre-treated with AA, AA-2 $\alpha$ G, or AA-2 $\beta$ G for 1 h, incubated with 10  $\mu\text{M}$  DCFH-DA or DHE for 30 min in serum free DMEM, and then stimulated with H<sub>2</sub>O<sub>2</sub> for 30 min. For detection of  $\Delta\Psi\text{m}$ , RAW264.7 cells were pre-treated with AA, AA-2 $\alpha$ G, or AA-2 $\beta$ G for 1 h, incubated with 10  $\mu\text{M}$  JC-1 at 37 °C for 30 min, and then stimulated with H<sub>2</sub>O<sub>2</sub> for 30 min. Changes in the fluorescent intensity of DCFH-DA, DHE, and JC-1 was determined using BD Accuri™ C6 flow cytometer (BD Biosciences, San Jose, CA, USA). At least 10,000 cells were recorded for each sample. The results were analyzed by using FlowJo software (TreeStar, San Carlos, CA, USA).

### 2.5. Lactate dehydrogenase (LDH) release assay

LDH released into the culture medium was determined using LDH Diagnostic kit (Beyotime Biotechnology, Shanghai, China). The absorbance was measured at 490 nm following the manufacture's recommendation (PerkinElmer, Waltham, MA, USA).

### 2.6. Detection of extracellular tumor necrosis factor (TNF)- $\alpha$ level

The level of secreted TNF- $\alpha$  in culture supernatant was measured with Multi-Analyte Flow Assay Kit (Biolegend, San Diego, CA, USA) using BD Accuri™ C6 flow cytometer according to the manufacturer's instructions.

### 2.7. Measurement of intracellular antioxidant enzyme activity

SOD, CAT, GSH, and GSSG activities in RAW264.7 cells were measured using commercially available assay kits from Beyotime according to the manufacturer's instructions.

### 2.8. Western blot analysis

At the end of the treatment, cells were lysed with ice-cold RIPA lysis buffer (Beyotime Biotechnology) supplemented with 1% PMSF and 1% protease inhibitor cocktail (Thermo Fisher Scientific, Rockford, IL, USA) on ice for 20 min. Cell lysate were cleared by centrifugation at 12,000 rpm for 15 min at 4 °C. Protein concentration was determined using Pierce® BCA Protein Assay Kit (Thermo Fisher Scientific). The samples were denatured by boiling in SDS loading buffer. Twenty  $\mu\text{g}$  of total protein was separated by 10% sodium dodecyl sulfate-polyacrylamide gel electrophoresis followed by electro blotting onto a polyvinylidene difluoride (PVDF) membrane (Bio-Rad, Hercules, CA, USA). After blocking in 5% nonfat milk dissolved in Tris-buffered saline-Tween 20 (TBS-T) buffer (20 mM Tris-HCl, pH 7.6, 150 mM NaCl, 0.1% Tween-20) for 1 h at room temperature, the membrane was probed with primary antibodies against Kelch-like ECH-associated protein-1 (Keap-1), nuclear factor E2-related factor 2 (Nrf2), heme oxygenase (HO)-1, and  $\beta$ -actin at 1:1,000 dilution in TBS-T overnight at 4 °C and specific secondary antibodies for 2 h at room temperature.

Specific protein bands were visualized using ECL advanced Western blot detection kit (GE Healthcare, Uppsala, Sweden).

### 2.9. Immunofluorescent staining

Immunofluorescent analysis was performed as previously reported [23]. In brief, RAW264.7 cells were fixed with 4% paraformaldehyde for 30 min, and blocked with 3% BSA in PBS for 1 h at room temperature. Cells were then incubated with primary antibody at optimal dilution in 3% BSA at 4 °C overnight followed by fluorescent conjugated secondary antibody at 1:500 dilution. Cells were then sealed in anti-fade reagent and examined under Leica TCS SP8 confocal microscope.

### 2.10. Nrf2 DNA binding activity assay

RAW264.7 cells were pre-treated with AA, AA-2 $\alpha$ G, or AA-2 $\beta$ G for 4 h, and then treated with 400  $\mu\text{M}$  H<sub>2</sub>O<sub>2</sub> for 6 h. Nuclear extract of RAW264.7 cells were prepared following the method reported previously [24]. Nrf2 promoter binding activity was measured using the Trans<sup>AM</sup> Nrf2 DNA-binding ELISA assay from Active Motif (Carlsbad, CA, USA) following the manufacture's recommendation.

### 2.11. ESI-QTOF-MS analysis

Cells were washed with PBS and harvested with methanol-water (v:v, 80:20). Equal number of cells were lysed by sonication and cleared by centrifugation at 15,000 rpm for 20 min at 4 °C. The intracellular content of AA, AA-2 $\alpha$ G, or AA-2 $\beta$ G were quantitatively analyzed using ESI-Q-TOF-MS/MS on a Bruker Impact HD Q-TOF MS system operating in ESI positive ion mode. The mass detection range was set as  $m/z$  100–1500 in the full scan mode. Samples were injected into the system and quantify with external standard dissolved in methanol-water (v:v, 80:20).

### 2.12. In vitro redox reaction

*In vitro* redox reaction was conducted with Fenton reagents [25]. In brief, 100  $\mu\text{L}$  of Fenton reagents was added to equal volume of AA, AA-2 $\alpha$ G, or AA-2 $\beta$ G in PBS. The change of absorbance was measured at 300 nm using FlexStation 5 multi-mode microplate reader (Molecular Devices, San Jose, CA, USA) every 3 min for a total of 30 min.

### 2.13. Statistical analysis

Data were presented as mean  $\pm$  SD from at least three independent experiments. Statistical significance between different experimental groups was determined by one-way analysis of variance (ANOVA) followed by Dunnett's post hoc test, and  $p$  values less than 0.05 was considered statistically significant.

## 3. Results

### 3.1. AA and its derivatives exhibited radical scavenging activity

We used H<sub>2</sub>O<sub>2</sub>-induced oxidative stress in murine M1/M2 macrophage RAW264.7 cells to determine the antioxidant activities of AA, AA-2 $\alpha$ G, and AA-2 $\beta$ G. None of these compounds alone affect cell viability as detected using MTT assay (Fig. 1B). Then, we then stimulated RAW264.7 cells with different concentrations of H<sub>2</sub>O<sub>2</sub>, and found that H<sub>2</sub>O<sub>2</sub> at 400  $\mu\text{M}$  began to trigger ROS considerably after 30 min (Fig. 1C). AA, AA-2 $\alpha$ G, and AA-2 $\beta$ G significantly reduced the DCFH-DA oxidation in H<sub>2</sub>O<sub>2</sub>-treated RAW264.7 cells in a dose-dependent manner (Fig. 1D). AA-2 $\alpha$ G at 50  $\mu\text{M}$  and AA-2 $\beta$ G at 12.5  $\mu\text{M}$  suppressed the H<sub>2</sub>O<sub>2</sub>-induced fluorescence of oxidized DHE to the same extent as 100  $\mu\text{M}$  AA (Fig. 1E). Treatment with H<sub>2</sub>O<sub>2</sub> decreased the ratio of JC-1 red to JC-1 green. Meanwhile, AA, AA-2 $\alpha$ G, and AA-2 $\beta$ G potently

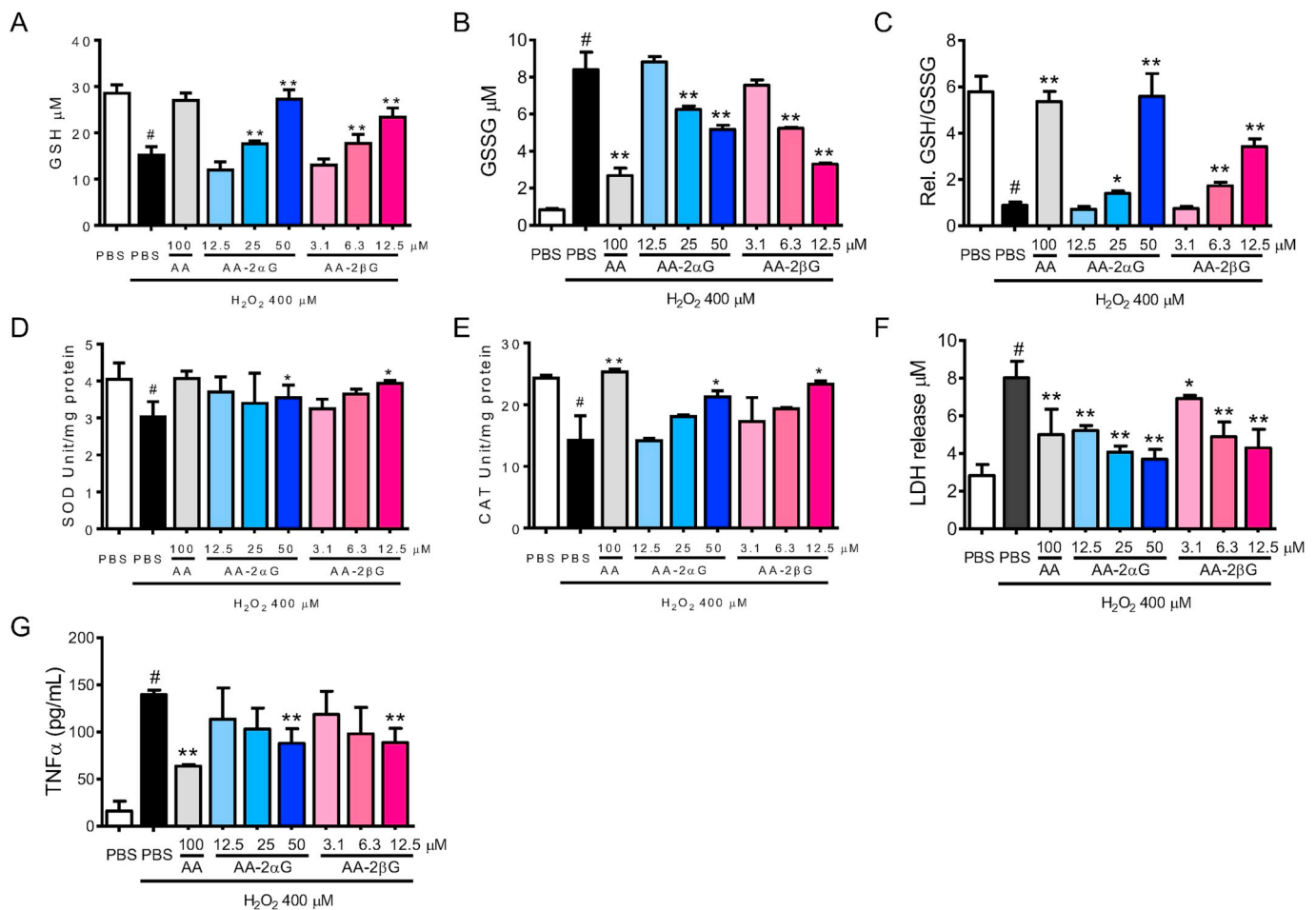


**Fig. 2.** AA, AA-2αG, and AA-2βG increased the intracellular antioxidant enzyme activity. RAW264.7 cells were pretreated with different of AA, AA-2αG, and AA-2βG concentrations for 4 h, followed by H<sub>2</sub>O<sub>2</sub> treatment for another 6 h. The effects on (A) GSH level, (B) GSSG level, (C) GSH/GSSG ratio, (D) SOD level, (E) CAT level, (F) LDH level and (G) TNF-α level released into the culture medium were determined using commercially available kits following the manufacturer's instruction. The results are presented as mean ± SD of the three separate experiments (\*,  $p < 0.05$  and \*\*,  $p < 0.01$  compared with H<sub>2</sub>O<sub>2</sub> treatment; #,  $p < 0.05$  compared with PBS treatment).

enhanced the ratio of JC-1 read to JC-1 green, thereby indicating that H<sub>2</sub>O<sub>2</sub>-reduced  $\Delta\Psi_m$  was restored by these compounds (Fig. 1F).

### 3.2. Treatments with AA, AA-2αG, and AA-2βG restored intracellular antioxidant enzyme activity and abrogated H<sub>2</sub>O<sub>2</sub>-induced cell death

Intracellular GSH depletes toxic radicals in acute oxidative stress. The recovery of the intracellular GSH content could relieve oxidative damage. Hydrogen peroxide challenge significantly depleted intracellular GSH level and increased the GSSG level, which decreased the ratio of GSH to GSSG compared with PBS-treated control group (Fig. 2A–C). Treatment with AA, AA-2αG, and AA-2βG significantly increased the GSH level and decreased the GSSG level, thereby enhancing the GSH-to-GSSG ratio (Fig. 2A–C). AA-2βG at 12.5 μM exhibited similar activity in restoring the GSH level but showed low potency in GSSG depletion, and hence increased the ratio of GSH to GSSG at 50 μM AA-2αG and 100 μM AA did (Fig. 2A–C). Superoxide dismutase (SOD) is an important metalloenzyme that specifically remove O<sub>2</sub><sup>-</sup> anions [26]. Catalase (CAT) catalyzes the decomposition of H<sub>2</sub>O<sub>2</sub>, thereby preventing oxidation [27]. Treatment with AA, AA-2αG, and AA-2βG ameliorated the suppressive effect of H<sub>2</sub>O<sub>2</sub> on SOD and CAT activities to levels comparative to those of PBS-treated control (Fig. 2D and E).

AA at 100 μM remarkably suppressed LDH (Fig. 2F) and TNF-α (Fig. 2G) release in H<sub>2</sub>O<sub>2</sub>-treated RAW264.7 cells. AA-2αG and AA-2βG potentially inhibited H<sub>2</sub>O<sub>2</sub>-triggered LDH (Fig. 2F) and TNF-α (Fig. 2G) release at 50 and 12.5 μM, respectively.

### 3.3. AA, AA-2αG, and AA-2βG prevented CPT-11-induced oxidative stress

Then, we extended to determine the antioxidant activities of AA, AA-2αG, and AA-2βG in chemotherapeutic agents-induced initial oxidative stress. The cytotoxic alkaloid agent CPT-11 at 10 μM and the nucleoside metabolic inhibitor 5-FU at 40 μM inhibited viability of RAW264.7 cells in a time-dependent manner (Fig. 3A–B). CPT-11 triggered remarkable ROS production (Fig. 3B); while 5-FU only induced significant substantial oxidation of DCFH-DA (Fig. 3B). Treatments with AA, AA-2αG, and AA-2βG significantly decreased CPT-11- but not 5-FU-triggered oxidation of DCFH-DA (Fig. 3C–D).

### 3.4. AA-2βG exhibited enhanced the Nrf2 DNA binding activity than AA and AA-2αG

We next determined the effects of AA, AA-2αG, and AA-2βG on the Keap-1/Nrf2 signaling pathway, which governs the transcription of several downstream antioxidant and detoxifying enzymes to eliminate intracellular radical [28]. The expression Keap-1 level stimulated by H<sub>2</sub>O<sub>2</sub> was downregulated with AA, AA-2αG, and AA-2βG treatments (Fig. 4A–B). Meanwhile, AA, AA-2αG, and AA-2βG significantly reversed the H<sub>2</sub>O<sub>2</sub>-suppressed Nrf2 and HO-1 expression levels (Fig. 4A–B). AA, AA-2αG, and AA-2βG induced the nuclear translocation of Nrf2 after H<sub>2</sub>O<sub>2</sub> stimulation (Fig. 4C) and enhanced the binding between Nrf2 and its targeting DNA sequence (Fig. 4D). In particular, AA-2βG at 12.5 μM exhibited approximately twofold higher potency in

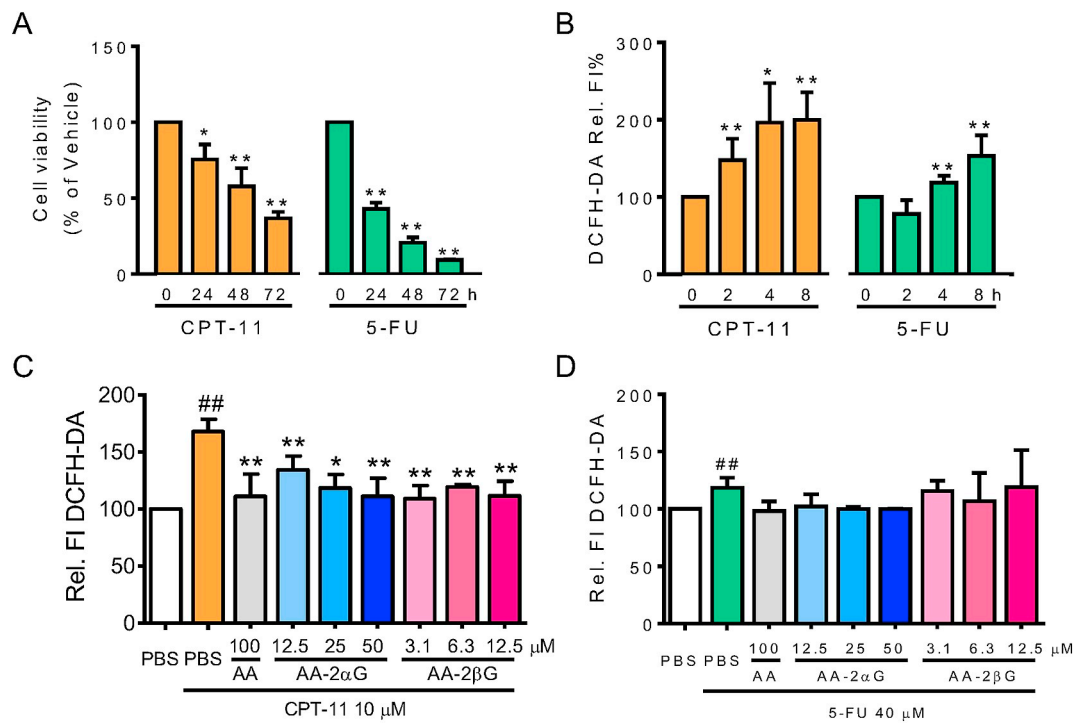


**Fig. 3.** Treatment with AA, AA-2 $\alpha$ G, and AA-2 $\beta$ G prevented CPT-11-induced ROS. (A) Cell viability of RAW264.7 cells treated with 10  $\mu$ M CPT-11 or 40  $\mu$ M 5-FU for up to 72 h. (B) ROS generation with CPT-11 or 5-FU treatment was analyzed with DCFH-DA staining. RAW264.7 cells were pretreated with different concentrations of AA, AA-2 $\alpha$ G, and AA-2 $\beta$ G for 1 h, followed by treatment with CPT-11 or 5-FU for the time indicated on the figure. ROS generation in (C) CPT-11 pretreatment for 2 h and (D) 5-FU pretreatment for 4 h were analyzed by DCFH-DA staining. The results are presented as mean  $\pm$  SD of the three separate experiments (\*,  $p < 0.05$  and \*\*,  $p < 0.01$  compared with H<sub>2</sub>O<sub>2</sub> treatment; #,  $p < 0.05$  compared with PBS treatment).

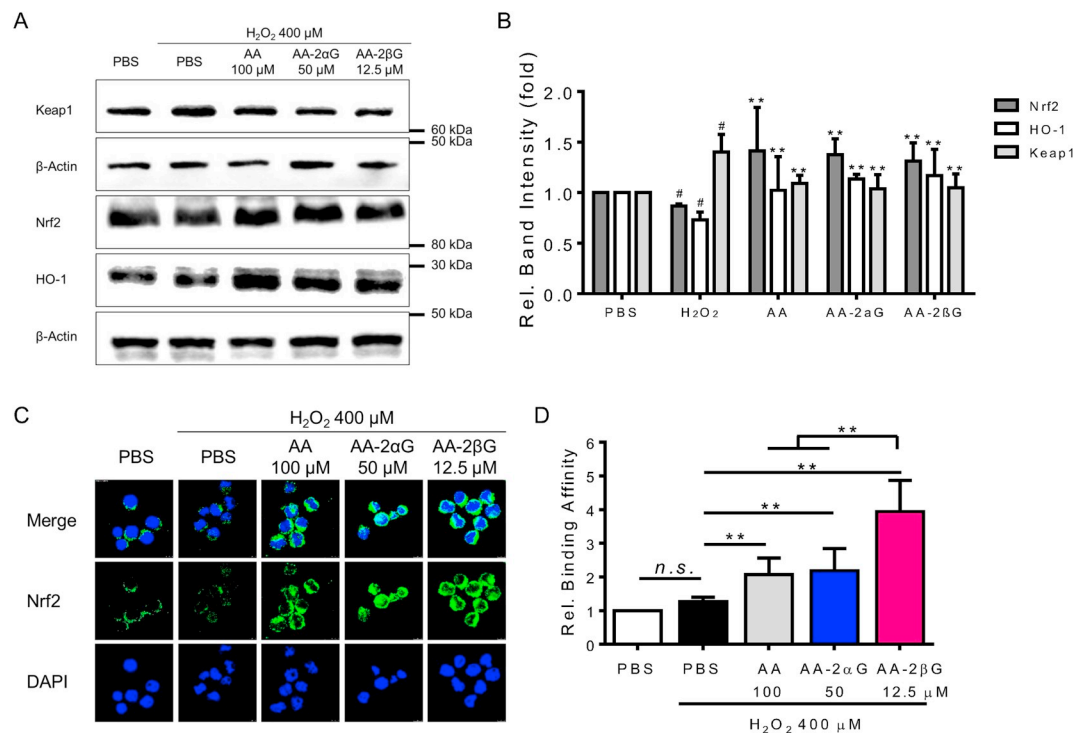


**Fig. 4.** AA, AA-2 $\alpha$ G, and AA-2 $\beta$ G activated the Nrf2 signaling pathway. RAW264.7 cells were pretreated with AA, AA-2 $\alpha$ G, and AA-2 $\beta$ G for 4 h, followed by H<sub>2</sub>O<sub>2</sub> treatment for another 6 h. (A) The expression levels of Keap-1, Nrf2, and HO-1 in RAW264.7 cells, and (B) the normalized band intensities of Keap-1, Nrf2, and HO-1 compared with that of  $\beta$ -actin. (C) Nuclear translocation of Nrf2 was detected with immunofluorescent staining. (D) Nrf2-DNA binding affinity of the nuclear extract from RAW264.7 cells pretreated with H<sub>2</sub>O<sub>2</sub> and then incubated with either PBS, AA, AA-2 $\alpha$ G, or AA-2 $\beta$ G. The binding of Nrf2 to its response element was determined using Trans<sup>AM</sup> Nrf2 kit following the manufacturer's recommendation. Results in (A) and (C) represent those of the three separate experiments. Results in (B) and (D) were presented as mean  $\pm$  SD from three separate experiments (\*\*,  $p < 0.01$  compared with H<sub>2</sub>O<sub>2</sub> treatment; #,  $p < 0.05$  compared with PBS treatment; n. s., not significant).



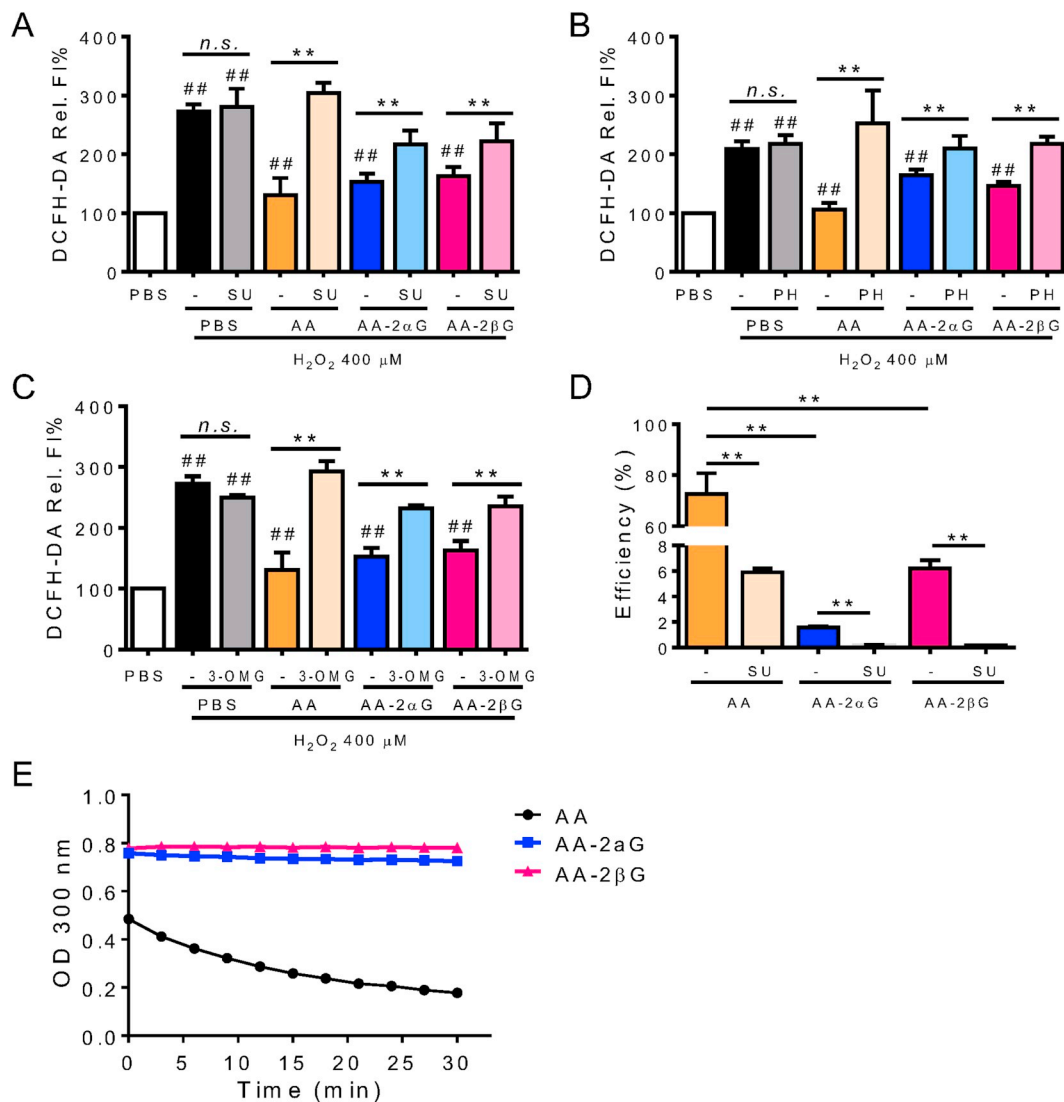


**Fig. 5.** Inhibition of SVCT abrogated the antioxidant activities of AA, AA-2αG, and AA-2βG. RAW264.7 cells were incubated with SVCT inhibitors (A) 5 μM SU, (B) 10 μM PH, and (C) 10 μM 3-OMG for 20 min and then pretreated with 100 μM AA, 50 μM AA-2αG, and 12.5 μM AA-2βG for 1 h, respectively. ROS generation was stimulated with 400 μM H<sub>2</sub>O<sub>2</sub> for 30 min, and determined using DCFH-DA staining. (D) RAW264.7 cells were preincubated with 5 μM SU for 20 min and then treated with AA and its derivative for 1 h similar to (A). The intracellular content of AA, AA-2αG, and AA-2βG contents were detected by ESI-QTOF-MS/MS. The uptake efficiency was calculated based on the total amount of each compound identified in the cell extract to the amount added in the culture medium. (E) *In vitro* stability of AA, AA-2αG, and AA-2βG in Fenton reagents for up to 30 min. Results are presented as mean ± SD from three separate times (\*,  $p < 0.05$  and \*\*,  $p < 0.01$  compared with H<sub>2</sub>O<sub>2</sub> treatment; #,  $p < 0.05$  compared with PBS treatment; n. s., not significant).

promoting Nrf2-DNA-binding activity than those of 100 μM AA and 50 μM AA-2αG (Fig. 4D).

### 3.5. Inhibition of SVCT and GLUT partially abrogated the antioxidant activity and cellular uptake of AA, AA-2αG, and AA-2βG

Pretreatment with the nonselective SVCT inhibitor SU and GLUT inhibitors PH and 3-OMG partially abrogated the abilities of AA, AA-2αG, and AA-2βG to decrease the level of oxidized DCFH-DA (Fig. 5A–C). Then, we measured the cellular uptake and possible oxidized product(s) of AA and its derivatives by using ESI-QTOF-MS/MS in RAW264.7 cells. The ESI-QTOF-MS/MS analysis results revealed that 70% of AA added into the culture medium was present in the cell lysate (Fig. 5D), while the uptake efficiency of AA-2αG and AA-2βG was ≤10% (Fig. 5D). We did not find any oxidized products of AA, or other metabolites of AA-2αG or AA-2βG in RAW 264.7 cells using ESI-QTOF-MS analysis (Fig. 6). The ferrous iron content suggested that approximately 50% of AA was oxidized after 30 min; while AA-2αG and AA-2βG remained in their reduced state *in vitro* (Fig. 5E).

## 4. Discussion

In the present study, we reported the excellent antioxidant activity of AA-2βG, which is a unique natural AA derivative identified in *L. barbarum*. The antioxidant activity of AA-2βG is related to activation of the Keap1/Nrf2 signaling pathway and SVCT-dependent cellular uptake. The presence of the D-glucosyl moiety on AA-2αG and AA-2βG prolonged their free radical scavenging activity but reduced their cellular uptake compared with AA. The β-configuration of AA-2βG also promoted the Nrf2-DNA-binding activity.

Antioxidants are used as food supplement to protect against the development of many types of aging-related diseases, maladaptive inflammation-induced macrophage death [29], and hematopoietic toxicity of chemotherapeutic agents. AA is one of the most easily accessible antioxidants from natural resources. AA exerts its scavenging activity mainly through direct redox reaction to restore the intracellular GSH pool [5]. The addition of the glucosyl group to AA-2αG and AA-2βG replaced the potentially oxidizable hydroxyl group on the C-2 position of

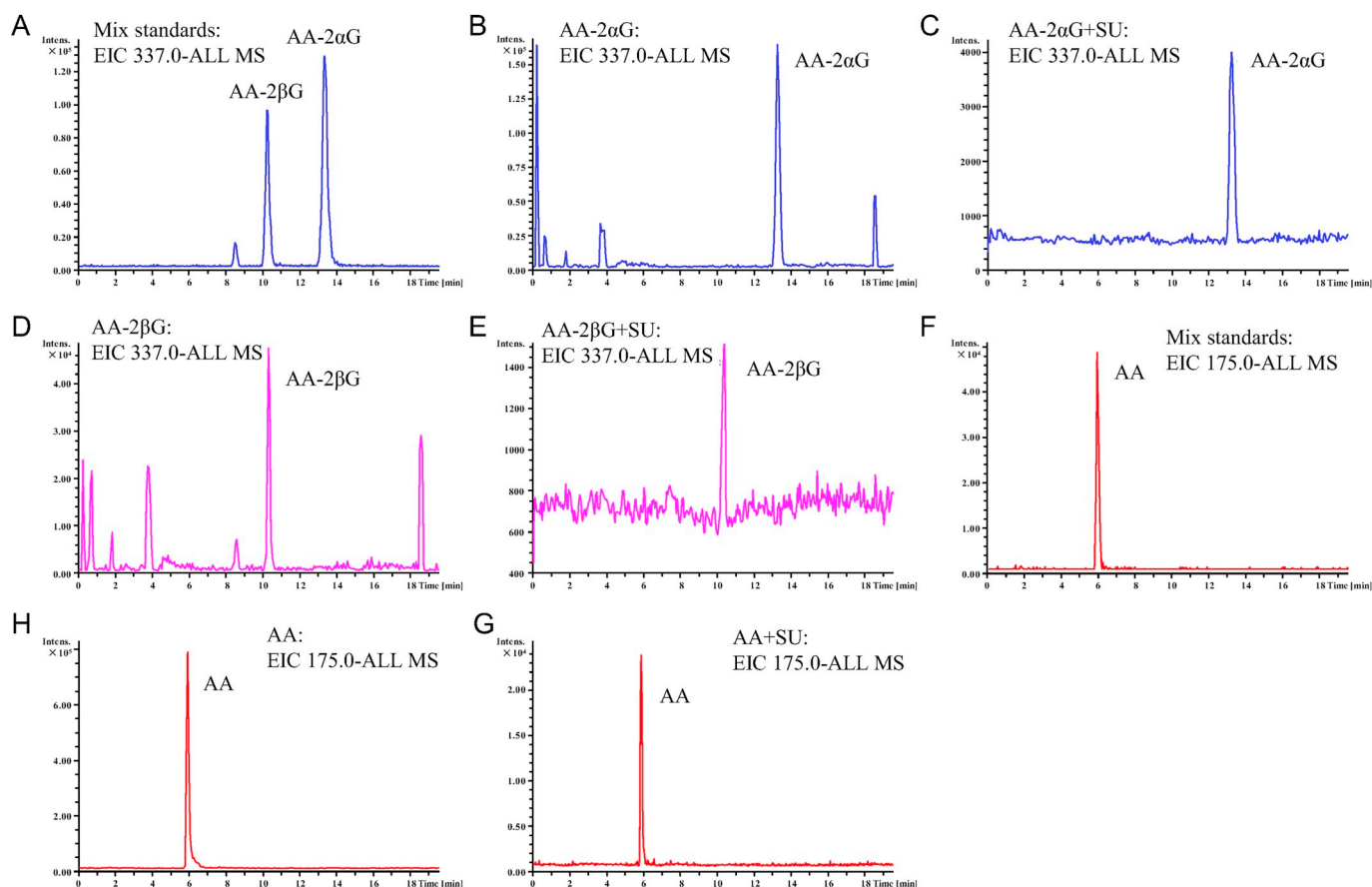


**Fig. 6.** ESI-QTOF-MS analysis spectrum of AA, AA-2 $\alpha$ G, AA-2 $\beta$ G. (A) AA-2 $\alpha$ G and AA-2 $\beta$ G standard. (B) AA-2 $\alpha$ G in RAW264.7 cell lysate. (C) AA-2 $\alpha$ G in cell lysate when RAW264.7 cells were pre-treated with 10  $\mu$ M sulfinpyrazone (SU). (D) AA-2 $\beta$ G in RAW264.7 cell lysate. (E) AA-2 $\beta$ G in cell lysate when RAW264.7 cells were pre-treated with 10  $\mu$ M SU. (F) AA standard. (G) AA in RAW264.7 cell lysate. Results are representative of three individual experiments.

AA. The lack of C-2 hydroxyl group may decrease the potent scavenging activities of AA-2 $\alpha$ G and AA-2 $\beta$ G on GSSG, SOD, and CAT levels in comparison to AA (Fig. 2A–E) [20]. This is in line with previous finding that baicalin exhibited higher radical scavenging activity than its aglycone baicalein [30]. AA-2 $\alpha$ G and AA-2 $\beta$ G were not metabolized to AA (Fig. 6). This may be due to the reason that RAW264.7 cells bare relatively low expression levels of  $\alpha$ - or  $\beta$ -glucosidase (data not show), thus could breakdown the glycosidic bond. These results suggested that AA-2 $\alpha$ G and AA-2 $\beta$ G may not quench free radicals through AA as intermediate but either through the activation of the cellular defense system or formation of covalent adduct with free radicals.

High AA concentration (10 g/day) is required to achieve the antioxidant capacity in overcoming its fast oxidation rate in the clinic [31]. High AA concentration is associated with increased kidney stone incidence and considerable renal, cardiac, and metabolic toxicity [8]. Several AA analogs have been synthesized to reduce the oxidation rate and increase stability. 6-O-Palmitoylascorbate, a lipophilic AA derivative, inhibits DNA damage and apoptotic cell death-induced by X-ray in submillimolar concentration [32,33]. The amphipathic AA derivative, 3-O-laurylglycerol ascorbate, maintains the free radical scavenging activity through the peroxisome proliferator activated receptor- $\gamma$  and Nrf2 signaling pathways [34]. AA-2 $\alpha$ G, which is widely used in the cosmetic and food industry as an antioxidant supplement, exhibits similar activity to that of AA in preventing H<sub>2</sub>O<sub>2</sub>-induced oxidative stress in dermal fibroblasts [35,36]. These AA derivatives are more stable than AA, but their potency are also similar to that of AA. The concentration required for AA-2 $\beta$ G to reduce direct DCFH-DA oxidation triggered by H<sub>2</sub>O<sub>2</sub> or CPT-11 was approximately 25% of that required for AA-2 $\alpha$ G (12.5  $\mu$ M vs 50  $\mu$ M) or 12% (12.5  $\mu$ M vs 100  $\mu$ M) required for AA (Figs. 1D and 3C). But AA and its derivatives exhibit no effect on

the initial substantial ROS induced by 5-FU (Fig. 3D), which was mediated through inhibition of DNA and RNA synthesis [37]. AA, AA-2 $\beta$ G, or AA-2 $\alpha$ G did not affect cell viability alone as detected by MTT assay (Fig. 1B) but abrogated H<sub>2</sub>O<sub>2</sub>-induced LDH and TNF- $\alpha$  release (Fig. 2F–G). MTT and LDH release assays are primarily based on intracellular redox reactions. Thus, the results may be affected by the antioxidant properties of AA, AA-2 $\beta$ G, or AA-2 $\alpha$ G. But fortunately TNF- $\alpha$  secretion was indirectly affected by intracellular ROS level. Therefore, AA-2 $\beta$ G or AA-2 $\alpha$ G exhibits enhanced free radical-scavenging activity per molecule against cell death compared with AA (Fig. 2F–G).

Antioxidants directly scavenge free radicals or reduce oxidative stress through restoration of the antioxidant defense mechanism. The fast oxidation rate suggested that AA directly interacts with free radicals (Fig. 5E). DHA, which is the oxidized product of AA, induces cell death in colorectal cancer carrying KRAS and BRAF mutation by deactivating glyceraldehyde 3-phosphate dehydrogenase [5]. The cytotoxic activity of DHA is also dependent upon its ability to induce oxidative stress by oxidizing GSH to GSSG [5,20]. Our results demonstrated that the controversial effect of AA as antioxidant in the clinic may be due to the metabolism and genetic background of the disease it was used to treat, and the high dose required. AA-2 $\alpha$ G activates the SIRT1 signaling pathway to delay the pathogenesis of dermal fibroblasts from H<sub>2</sub>O<sub>2</sub>-induced oxidative damage and cellular senescence [36]. AA-2 $\alpha$ G maintains the integrity of gastric epithelial cells from *Helicobacter pylori*-initiated mitochondrial death signaling [38]. We also proposed that the Keap-1/Nrf2 signaling is at least partially activated with AA, AA-2 $\alpha$ G, and AA-2 $\beta$ G treatment (Fig. 4).

SVCT and GLUT are generally recognized as rate limiting factors and universal transporters for AA in different cell types [5,39]. Intracellular AA also increases SVCT expression and its membrane

localization, which further promotes AA uptake [39,40]. Inhibition of SVCT or GLUT abrogated the antioxidant activity (Fig. 5A–C) and reduced the cellular uptake (Fig. 5D) of AA, AA-2 $\alpha$ G, or AA-2 $\beta$ G (Fig. 5A–D). This is in line that glucose conjugation did not change the physical or chemical activities of platinum (II) drugs and maintained their cellular target and active pharmacophore [41,42]. The concentration of AA-2 $\beta$ G to reduce oxidized DCFHDA was only 25% to that of AA-2 $\alpha$ G (compare 12.5  $\mu$ M–50  $\mu$ M on Fig. 5D); while, the cellular uptake efficiency of AA-2 $\beta$ G was approximately threefold to that of AA-2 $\alpha$ G (Fig. 5D). Thus, the intracellular AA-2 $\alpha$ G and AA-2 $\beta$ G are of similar concentrations. AA-2 $\beta$ G exhibited the same direct radical scavenging activity in the Fenton reagent (Fig. 5E), two fold activity in promoting Nrf2-DNA binding (Fig. 4D), and approximately 50% activity in restoration of intracellular GSH/GSSG (Fig. 2C) to AA-2 $\alpha$ G. Thus, the  $\beta$ - but not the  $\alpha$ -configuration of the glucosyl group favors activation of antioxidant genes instead of direct radical scavenging activity. The stability of AA-2 $\alpha$ G and AA-2 $\beta$ G was much higher than that of AA in the Fenton reagent (Fig. 5E), thus less AA-2 $\alpha$ G or AA-2 $\beta$ G is required to reduce free radicals than AA (Fig. 1D–E, 3C).

In summary, the study showed the following results: (1) the reactivity against free radical followed the order of AA-2 $\beta$ G > AA-2 $\alpha$ G > AA; (2) AA-2 $\alpha$ G and AA-2 $\beta$ G were not metabolized into AA in RAW264.7 cells, thereby suggesting that their antioxidant activity may not require AA as intermediate; (3) AA-2 $\alpha$ G and AA-2 $\beta$ G shared the same cellular uptake transporters as AA; and (4) the glucosyl moiety and its configuration on AA-2 $\beta$ G increased stability and enhanced the Nrf2-DNA-binding affinity. Here, AA-2 $\beta$ G can be used as a highly reactive antioxidant for the prevention of chemotherapeutic agents-induced damage and other free radical-triggered diseases.

## Declaration of conflicts

The authors declare no conflict of interests.

## Appendix A. Supplementary data

Supplementary data to this article can be found online at <https://doi.org/10.1016/j.redox.2019.101173>.

## Funding sources

This study was partially supported by the Macau Science and Technology Development Fund FDCT 0075/2018/A2 to SPL, and Research Fund of the University of Macao MYRG 2016-00105-ICMS-QRCM, and MYRG 2017-00116-ICMS-QRCM to YW.

## References

- [1] D. Karunakaran, M. Geoffrion, L. Wei, W. Gan, L. Richards, P. Shangari, E.M. DeKemp, R.A. Beanlands, L. Perisic, L. Maegdefessel, Targeting macrophage necroptosis for therapeutic and diagnostic interventions in atherosclerosis, *Sci. Adv.* 2 (2016) e1600224.
- [2] S. Hajra, A. Basu, S. Singha Roy, A.R. Patra, S. Bhattacharya, Attenuation of doxorubicin-induced cardiotoxicity and genotoxicity by an indole-based natural compound 3, 3'-diindolylmethane (DIM) through activation of Nrf2/ARE signaling pathways and inhibiting apoptosis, *Free Radic. Res.* 51 (2017) 812–827.
- [3] N. Shenoy, E. Creagan, T. Witzig, M. Levine, Ascorbic acid in cancer treatment: let the phoenix fly, *Cancer Cell* 34 (2018) 700–706.
- [4] C. Cheignon, M. Tomas, D. Bonnefont-Rousselot, P. Faller, C. Hureau, F. Collin, Oxidative stress and the amyloid beta peptide in Alzheimer's disease, *Redox Biol.* 14 (2018) 450–464.
- [5] J. Yun, E. Mullarky, C. Lu, K.N. Bosch, A. Kavalier, K. Rivera, J. Roper, I.I.C. Chio, E.G. Giannopoulou, C. Rago, Vitamin C selectively kills KRAS and BRAF mutant colorectal cancer cells by targeting GAPDH, *Science* 350 (2015) 1391–1396.
- [6] J. van der Reest, E. Gottlieb, Anti-cancer effects of vitamin C revisited, *Cell Res.* 26 (2016) 269.
- [7] J. Kirk, D. Dennison, P. Kokoczk, D. Heldman, Degradation of ascorbic acid in a dehydrated food system, *J. Food Sci.* 42 (1977) 1274–1279.
- [8] J.D. Schoenfeld, Z.A. Sibenaller, K.A. Mapuskar, B.A. Wagner, K.L. Cramer-Morales, M. Furqan, S. Sandhu, T.L. Carlisle, M.C. Smith, T.A. Hejleh, O2- and H2O2-mediated disruption of Fe metabolism causes the differential susceptibility of NSCLC and GBM cancer cells to pharmacological ascorbate, *Cancer Cell* 31 (2017) 487–500 e488.
- [9] H. Amagase, N.R. Farnsworth, A review of botanical characteristics, phytochemistry, clinical relevance in efficacy and safety of Lycium barbarum fruit (Goji), *Food Res. Int.* 44 (2011) 1702–1717.
- [10] Y. Toyoda-Ono, M. Maeda, M. Nakao, M. Yoshimura, N. Sugiura-Tomimori, H. Fukami, 2-O-( $\beta$ -D-Glucopyranosyl) ascorbic acid, a novel ascorbic acid analogue isolated from Lycium fruit, *J. Agric. Food Chem.* 52 (2004) 2092–2096.
- [11] H.-Y. Li, Y.-W. Ruan, P.W.-F. Kau, K. Chiu, R.C.-C. Chang, H.H. Chan, K.-F. So, Effect of Lycium barbarum (Wolfberry) on alleviating axonal degeneration after partial optic nerve transection, *Cell Transplant.* 24 (2015) 403–417.
- [12] Y. Sun, J. Rukeya, W. Tao, P. Sun, X. Ye, Bioactive compounds and antioxidant activity of wolfberry infusion, *Sci. Rep.* 7 (2017) 40605.
- [13] S. Wang, J.H. Suh, X. Zheng, Y. Wang, C.-T. Ho, Identification and quantification of potential anti-inflammatory hydroxycinnamic acid amides from wolfberry, *J. Agric. Food Chem.* 65 (2017) 364–372.
- [14] R.C.-C. Chang, K.-F. So, Use of anti-aging herbal medicine, Lycium barbarum, against aging-associated diseases. What do we know so far? *Cell. Mol. Neurobiol.* 28 (2008) 643–652.
- [15] A. Mocan, L. Vlase, D.C. Vodnar, C. Bischin, D. Hanganu, A.-M. Gheldiu, R. Oprean, R. Silaghi-Dumitrescu, G. Crişan, Polyphenolic content, antioxidant and antimicrobial activities of Lycium barbarum L. and Lycium chinense Mill. leaves, *Molecules* 19 (2014) 10056–10073.
- [16] J.-H. Xie, W. Tang, M.-L. Jin, J.-E. Li, M.-Y. Xie, Recent advances in bioactive polysaccharides from Lycium barbarum L., Zizyphus jujuba Mill, Plantago spp., and Morus spp.: structures and functionalities, *Food Hydrocolloids* 60 (2016) 148–160.
- [17] X. Li, X. Li, A. Zhou, Evaluation of antioxidant activity of the polysaccharides extracted from Lycium barbarum fruits in vitro, *Eur. Polym. J.* 43 (2007) 488–497.
- [18] G. Xin, F. Zhu, B. Du, B. Xu, Antioxidants distribution in pulp and seeds of black and red goji berries as affected by boiling processing, *J. Food Qual.* (2017) 2017.
- [19] Y. Toyada-Ono, M. Maeda, M. Nakao, M. Yoshimura, N. Sugiura-Tomimori, H. Fukami, H. Nishioka, Y. Miyashita, S. Kojo, A novel vitamin C analog, 2-O-( $\beta$ -D-Glucopyranosyl) ascorbic acid: examination of enzymatic synthesis and biological activity, *J. Biosci. Bioeng.* 99 (2005) 361–365.
- [20] J. Takebayashi, Y. Yagi, R. Ishii, S. Abe, K. Yamada, A. Tai, Antioxidant properties of 2-O- $\beta$ -D-glucopyranosyl-L-ascorbic acid, *Biosci. Biotechnol. Biochem.* 72 (2008) 1558–1563.
- [21] S.C. Lam, Z. Luo, D.T. Wu, K.L. Cheong, D.J. Hu, Z.M. Xia, J. Zhao, S.P. Li, Comparison and characterization of compounds with antioxidant activity in Lycium barbarum using high-performance thin layer chromatography coupled with DPPH bioautography and tandem mass spectrometry, *J. Food Sci.* 81 (2016) C1378–C1384.
- [22] Z. Zhang, X. Liu, X. Zhang, J. Liu, Y. Hao, X. Yang, Y. Wang, Comparative evaluation of the antioxidant effects of the natural vitamin C analog 2-O- $\beta$ -D-glucopyranosyl-L-ascorbic acid isolated from Goji berry fruit, *Arch Pharm. Res. (Seoul)* 34 (2011) 801–810.
- [23] X. Nie, S.-R. Chen, K. Wang, Y. Peng, Y.-T. Wang, D. Wang, Y. Wang, G.-C. Zhou, Attenuation of innate immunity by andrographolide derivatives through NF- $\kappa$ B signaling pathway, *Sci. Rep.* 7 (2017) 4738.
- [24] Y. Wang, S. Lee, Y. Ha, W. Lam, S.-R. Chen, G.E. Dutschman, E.A. Gullen, S.P. Grill, Y. Cheng, A. Fürstner, Tylophorine analogs allosterically regulates heat shock cognate protein 70 and inhibits hepatitis C virus replication, *Sci. Rep.* 7 (2017) 10037.
- [25] R.V. Lloyd, P.M. Hanna, R.P. Mason, The origin of the hydroxyl radical oxygen in the Fenton reaction, *Free Radical Biol. Med.* 22 (1997) 885–888.
- [26] J.M. McCord, I. Fridovich, Superoxide dismutase an enzymic function for erythrocyte hemocuprein (hemocuprein), *J. Biol. Chem.* 244 (1969) 6049–6055.
- [27] M.M. Goyal, A. Basak, Human catalase: looking for complete identity, *Protein Cell* 1 (2010) 888–897.
- [28] M. Danilenko, G.P. Studzinski, Keep harm at bay: oxidative phosphorylation induces Nrf2-driven antioxidant response via ERK5/MEF2/miR-23a signaling to Keap-1, *EBioMedicine* 3 (2016) 4–5.
- [29] D. Karunakaran, M. Geoffrion, L. Wei, W. Gan, L. Richards, P. Shangari, E.M. DeKemp, R.A. Beanlands, L. Perisic, L. Maegdefessel, U. Hedin, S. Sad, L. Guo, F.D. Kolodgie, R. Virmani, T. Ruddy, K.J. Rayner, Targeting macrophage necroptosis for therapeutic and diagnostic interventions in atherosclerosis, *Sci. Adv.* 2 (2016) e1600224.
- [30] B. Dinda, S. Dinda, S. DasSharma, R. Banik, A. Chakraborty, M. Dinda, Therapeutic potentials of baicalin and its aglycone, baicalein against inflammatory disorders, *Eur. J. Med. Chem.* 131 (2017) 68–80.
- [31] E. Cameron, A. Campbell, T. Jack, The orthomolecular treatment of cancer: III. Reticulum cell sarcoma: double complete regression induced by high-dose ascorbic acid therapy, *Chem. Biol. Interact.* 11 (1975) 387–393.
- [32] L. Xiao, T. Tsutsui, N. Miwa, The lipophilic vitamin C derivative, 6-O-palmitoylascorbate, protects human lymphocytes, preferentially over ascorbate, against X-ray-induced DNA damage, lipid peroxidation, and protein carbonylation, *Mol. Cell. Biochem.* 394 (2014) 247–259.
- [33] L. Xiao, N. Miwa, The lipophilic vitamin C derivative, 6-O-palmitoylascorbate protects human keratinocytes and 3d-human skin equivalents against X-ray-induced oxidative stress and apoptosis more markedly than L-ascorbic acid, *J. Cell. Biochem.* 118 (2017) 318–329.
- [34] Y. Katsuyama, T. Tsuboi, N. Taira, M. Yoshioka, H. Masaki, 3-O-Laurylglycerol ascorbate activates the intracellular antioxidant system through the contribution of PPAR- $\gamma$  and Nrf2, *J. Dermatol. Sci.* 82 (2016) 189–196.
- [35] M. Taniguchi, N. Arai, K. Kohno, S. Ushio, S. Fukuda, Anti-oxidative and anti-aging activities of 2-O- $\alpha$ -glucopyranosyl-L-ascorbic acid on human dermal fibroblasts,



- Eur. J. Pharmacol. 674 (2012) 126–131.
- [36] M. Taniguchi, N. Arai, K. Kohno, S. Ushio, S. Fukuda, Anti-oxidative and anti-aging activities of 2-O-alpha-glucopyranosyl-L-ascorbic acid on human dermal fibroblasts, *Eur. J. Pharmacol.* 674 (2012) 126–131.
- [37] J. Kanterman, M. Sade-Feldman, M. Biton, E. Ish-Shalom, A. Lasry, A. Goldshtein, A. Hubert, M. Baniyash, Adverse immunoregulatory effects of 5FU and CPT11 chemotherapy on myeloid-derived suppressor cells and colorectal cancer outcomes, *Cancer Res.* 74 (2014) 6022–6035.
- [38] X. Chen, R. Liu, X. Liu, C. Xu, X. Wang, L-ascorbic Acid-2-Glucoside inhibits *Helicobacter pylori*-induced apoptosis through mitochondrial pathway in Gastric Epithelial cells, *Biomed. Pharmacother.* 97 (2018) 75–81.
- [39] S.A. Mason, P.A. Della Gatta, R.J. Snow, A.P. Russell, G.D. Wadley, Ascorbic acid supplementation improves skeletal muscle oxidative stress and insulin sensitivity in people with type 2 diabetes: findings of a randomized controlled study, *Free Radic. Biol. Med.* 93 (2016) 227–238.
- [40] A. Covarrubias-Pinto, A.I. Acuna, G. Boncompain, E. Papic, P.V. Burgos, F. Perez, M.A. Castro, Ascorbic acid increases SVCT2 localization at the plasma membrane by accelerating its trafficking from early secretory compartments and through the endocytic-recycling pathway, *Free Radic. Biol. Med.* 120 (2018) 181–191.
- [41] J. Ma, Q. Wang, Z. Huang, X. Yang, Q. Nie, W. Hao, P.G. Wang, X. Wang, Glycosylated platinum(IV) complexes as substrates for glucose transporters (GLUTs) and organic cation transporters (OCTs) exhibited cancer targeting and human serum albumin binding properties for drug delivery, *J. Med. Chem.* 60 (2017) 5736–5748.
- [42] Q.L. He, I. Minn, Q. Wang, P. Xu, S.A. Head, E. Datan, B. Yu, M.G. Pomper, J.O. Liu, Targeted delivery and sustained antitumor activity of triptolide through glucose conjugation, *Angew Chem. Int. Ed. Engl.* 55 (2016) 12035–12039.